

# Near-infrared imaging of developmental defects in dental enamel

Krista Hirasuna

Daniel Fried

Cynthia L. Darling

University of California, San Francisco  
San Francisco, California 94143-0758

**Abstract.** Polarization-sensitive optical coherence tomography (PS-OCT) and near-infrared (NIR) imaging are promising new technologies under development for monitoring early carious lesions. Fluorosis is a growing problem in the United States, and the more prevalent mild fluorosis can be visually mistaken for early enamel demineralization. Unfortunately, there is little quantitative information available regarding the differences in optical properties of sound enamel, enamel developmental defects, and caries. Thirty extracted human teeth with various degrees of suspected fluorosis were imaged using PS-OCT and NIR. An InGaAs camera and a NIR diode laser were used to measure the optical attenuation through transverse tooth sections ( $\sim 200 \mu\text{m}$ ). A digital microradiography system was used to quantify the enamel defect severity by measurement of the relative mineral loss for comparison with optical scattering measurements. Developmental defects were clearly visible in the polarization-resolved OCT images, demonstrating that PS-OCT can be used to nondestructively measure the depth and possible severity of the defects. Enamel defects on whole teeth that could be imaged with high contrast with visible light were transparent in the NIR. This study suggests that PS-OCT and NIR methods may potentially be used as tools to assess the severity and extent of enamel defects. © 2008 Society of Photo-Optical Instrumentation Engineers. [DOI: 10.1117/1.2956374]

**Keywords:** near-infrared (NIR) imaging; polarization-sensitive optical coherence tomography (PS-OCT); developmental defects; fluorosis; attenuation coefficients.

Paper 07445R received Nov. 2, 2007; revised manuscript received Feb. 11, 2008; accepted for publication Mar. 10, 2008; published online Jul. 28, 2008. This paper is a revision of a paper presented at the SPIE conference on Lasers in Dentistry XIII, January 2007, San Jose, California. The paper presented there appears (unrefereed) in SPIE Proceedings Vol. 6425.

## 1 Introduction

Over the past 50 years, the nature of dental decay or dental caries in the United States has changed due to the introduction of fluoride to the drinking water, use of fluoride dentifrices and rinses, application of fluoride topicals in the dental office, and improved dental hygiene. With the increase of fluoride use, the prevalence of caries has been reduced, but fluorosis has become a growing problem. Fluorosis is the hypomineralization of enamel due to fluoride ingestion during tooth development (first 6 years of life for most permanent teeth). Enamel fluorosis is characterized by greater surface and subsurface porosity.<sup>1</sup> The Centers for Disease Control (CDC) recently published a report, showing a 9% higher prevalence of fluorosis in American children than was found in a similar study 20 years ago.<sup>2</sup> Recent estimates show that fluorosis affects an average of 48% of children in fluoridated communities,<sup>3</sup> an almost five-fold increase from the 1940s.

Severe fluorosis can be readily distinguished, but the more common mild fluorosis can be easily mistaken for early

enamel demineralization due to caries. The differentiation between fluorotic and nonfluorotic enamel defects is an important diagnostic decision for epidemiology and public health dentistry. Numerous studies have looked at the optical properties of early carious lesions and demineralized enamel, but there appear to be no attempts to measure the optical properties of hypomineralized enamel in developmental defects such as fluorosis.

Currently, fluorosis is scored based on color and tooth morphology commonly using the Thylstrup-Fejerskov (TF) index or Dean's fluorosis index.<sup>1</sup> Most cases of fluorosis can be identified using these criteria. However, it has not been confirmed that the pattern and distribution of the lesions due to fluorosis are a unique occurrence. Angmar-Mansson et al.<sup>4</sup> researched several optical techniques for improving the assessment of dental fluorosis. According to Angmar-Mansson et al.,<sup>4</sup> mild enamel fluorosis is characterized clinically by "diffuse opacities. The appearance is due to optical properties of a subsurface or surface porous layer with lower mineral content. These areas usually have texture and color similar to those of initial caries lesions but generally another shape and location." They conclude that a light-scattering monitor can

Address all correspondence to Daniel Fried, Univ. of California, San Francisco, San Francisco, CA 94143-0758. Tel: 415-502-6641; Fax: 415-476-0858; E-mail: daniel.fried@ucsf.edu

be used to determine the local porosity of the fluorotic enamel and that laser fluorescence may be developed into a method to evaluate the severity of the enamel fluorosis.<sup>4</sup> Quantitative light-induced fluorescence has been used as a potential diagnostic tool for fluorosis because the subsurface porosities scatter light in a similar manner to demineralized carious lesions.<sup>5</sup>

Our previous work involving near-infrared (NIR) imaging demonstrated that the high transparency of enamel in this region can be exploited to image occlusal and interproximal lesions via transillumination of the tooth.<sup>6–10</sup> Other studies have shown that there is an exponential increase in light scattering corresponding to increasing mineral loss in enamel caries, and that the scattering coefficient increases by almost two orders of magnitude at 1310 nm.<sup>11,12</sup> Differences in appearance between demineralization from caries and hypomineralization from developmental defects in some initial NIR images suggest that it may be possible to differentiate between developmental defects and demineralization in the NIR.<sup>13</sup>

Optical coherence tomography (OCT) is a noninvasive technique for creating cross-sectional images of internal biological structure.<sup>14–18</sup> Polarization-sensitive OCT (PS-OCT) at 1310 nm has been shown to be effective in imaging dental caries and early lesions.<sup>19–21</sup> but there is no data showing its effectiveness in differentiating between hypomineralized and demineralized enamel. Moreover, it is likely that if there are differences in the optical behavior between demineralization from caries and hypomineralization from developmental defects in the NIR, those differences should be visible in OCT images.

In this paper, we present NIR and PS-OCT images of teeth with suspected developmental defects likely due to fluorosis. In addition, the attenuation of NIR light at 1310 nm was measured as a function of mineral loss to determine whether there are differences in the optical behavior of demineralization from caries and hypomineralization from developmental defects in the NIR. These initial results suggest that PS-OCT may be used as a tool to assess the severity and extent of fluorotic lesions and that NIR imaging methods hold considerable promise for the differentiation of mild fluorosis from early carious lesions.

## 2 Materials and Methods

### 2.1 Sample Preparation

Extracted molars and bicuspids extracted for orthodontic reasons were obtained from patients in the San Francisco Bay Area. Tooth collection was approved by the University of California, San Francisco Committee on Human Research. The teeth were cleaned and sterilized with gamma radiation and kept in a (0.1% thymol) solution to prevent fungal and bacterial growth. Thirty teeth with suspected hypomineralization and/or demineralization from caries were chosen based on visual inspection. Teeth were chosen by developmental defect location—lingual and facial defects were preferred to interproximal lesions, and defects on the cusp tips were preferred to lesions in the grooves and fissures. These criteria were intended to increase the probability of selecting teeth with fluorosis and not caries. Dean's fluorosis index was used to obtain teeth with various degrees of enamel fluorosis.<sup>1</sup>

All thirty teeth were mounted on  $1.2 \times 1.2 \times 3$  cm<sup>3</sup> rectangular blocks of black orthodontic composite resin with the

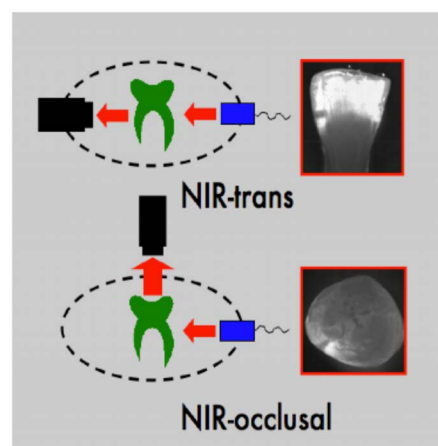


**Fig. 1** NIR imaging setup for NIR-trans (top) and NIR-occlusal (bottom) of tooth.

occlusal surface facing out from the square surface of the block. Each rectangular block fit precisely in an optomechanical assembly that could be positioned with micron accuracy. The rectangular symmetry of the mount facilitates matching the position of plano-parallel OCT scans to the thin sections produced for future mineral density determination using digital transverse microradiography (TMR).

### 2.2 NIR Imaging

The NIR imaging setup is shown schematically in Fig. 1. Light from a single-mode fiber-pigtail coupled to a 1310-nm superluminescent diode (SLD) with an output power of 15 mW and a 35-nm bandwidth, Model SLED1300D20A (Optospeed, Zurich, Switzerland), was used as the illuminating source. We found that broadband SLDs were advantageous to avoid speckle. An InGaAs focal plane array (FPA) (318 × 252 pixels) the Alpha NIR (Indigo Systems, Goleta, California) with a Infinimite video lens (Infinity, Boulder, Colorado) was used to acquire all images. The acquired 12-bit digital images were analyzed using IR Vista software (Indigo Systems, Goleta, California). Two modes of imaging were used for imaging decay on proximal and occlusal surfaces that we call NIR-trans and NIR-occlusal mode imaging, as illustrated in Fig. 1.

The NIR-trans mode of collecting NIR images is shown schematically in Fig. 1. In the NIR-trans mode images, the broadband light source and the InGaAs FPA are opposite each other, and crossed NIR polarizers, Model K46-252 (Edmund Scientific, Barrington, New Jersey), were inserted to remove light that directly illuminated the array without passing through the tooth.<sup>22</sup>

For NIR-occlusal mode imaging, light enters the teeth just above the gumline and is highly scattered by the dentin. The diffusely scattered light migrates upward toward the surface of the crown, into the occlusal surface of the tooth. The enamel of the crown (outer white area) is transparent at 1310 nm and varies from 1 to 3 mm in thickness.<sup>23</sup>

Reflected light images in the visible range were acquired of each occlusal surface using a color 1/3 in. CCD camera

with a resolution of 450 lines, Model DFK 5002/N (Imaging Source, Charlotte, North Carolina), equipped with the same Infinimite video lens.

### 2.3 Polarization-Sensitive Optical Coherence Tomography

An all single-mode fiber autocorrelator-based optical coherence domain reflectometry (OCDR) system with polarization switching probe, high-efficiency piezoelectric fiber-stretchers, and an InGaAs receiver that was fabricated by Optiphase, Inc. (Van Nuys, California), was used to acquire images of the occlusal and smooth surface tomography of hypomineralized and demineralized teeth. This OCDR system was coupled with a broadband high-power superluminescent diode (SLD) from Denselight (Jessup, Maryland) with an output power of 10 mW and a bandwidth of 83 nm for a spatial resolution of 12  $\mu\text{m}$  in air and 7.5  $\mu\text{m}$  in enamel. A high-speed XY-scanning system with an ESP 300 controller and 850G-HS stages from National Instruments (Austin, Texas) was integrated with the SLD for *in vitro* optical tomography. The probe was designed to provide a spot diameter of 50  $\mu\text{m}$  over a range of 10 mm. The system has been described in greater detail in Refs. 24 and 25. The PS-OCT system was controlled using Labview software from National Instruments (Austin, Texas). The intensity of backscattered light was measured as a function of depth within the tissue. Two-dimensional (2-D) OCT intensity plots were obtained by laterally scanning the beam across the tooth.

### 2.4 Digital Microradiography

A custom-built digital microradiography (TMR) system was used to measure the volume percent mineral content in the areas of hypomineralization on the tooth sections. High-resolution microradiographs were taken using Cu  $K_{\alpha}$  radiation from a Philips 3100 x-ray generator and a Photonics Science FDI x-ray digital imager (Microphotonics, Allentown, Pennsylvania). The x-ray digital imager consists of a 1392  $\times$  1040 pixel interline CCD directly bonded to a coherent micro fiber-optic coupler that transfers the light from an optimized gadolinium oxysulphide scintillator to the CCD sensor. The pixel resolution is 2.1  $\mu\text{m}$ , and images can be acquired in real time at a frame rate of 10 fps. A high-speed motion control system with Newport UTM150 and 850G stages and an ESP 300 controller coupled to a video microscopy and laser targeting system was used for precise positioning of the tooth sample in the field of view of the imaging system. The experimental setup is shown in Ref. 12.

## 3 Results

### 3.1 NIR Imaging of Developmental Defects

Figures 2–4 show visible and NIR images of four teeth with developmental defects. In Fig. 2, two teeth are shown, comparing images taken in visible reflected light and NIR transillumination (NIR-trans mode of Fig. 1). The first tooth of Figs. 2(a) and 2(b) shows a large stained defect with the defect visible over a large portion of the tooth crown. In contrast, the NIR image shows the lesion over three more highly localized areas. There are differences between the visible and NIR images, and the NIR images show only the most severe areas of

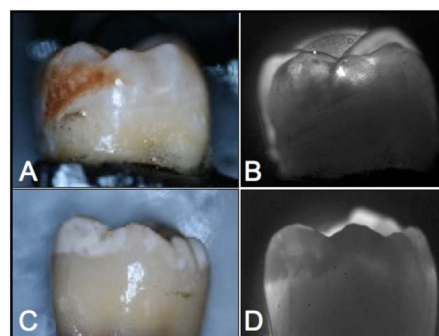


**Fig. 2** Visible reflected light images (a) and (c) and NIR-trans images (b) and (d) of two teeth covered by mild and moderate developmental defects. Note the “white caps” in (a) and (c), characteristic of teeth with developmental defects due to fluorosis.

decay in the NIR-trans imaging mode. PS-OCT images of the same tooth along with images of a histological thin section are shown in Fig. 5 and indicate that the opaque areas in the NIR-trans image match the areas of deep penetration of the defect into the enamel while the areas of shallow penetration are not visible in the NIR-trans images. In the second tooth, Figs. 2(c) and 2(d), the visible and NIR images are a better match, and both images show the defect over most of the upper part of the crown of that tooth.

The most interesting contrast between the visible light and NIR images is provided by the occlusal views. In Fig. 3, we have buccal and occlusal reflected visible light images of a molar with “white caps,” most likely due to hypomineralization. The tooth is also heavily stained on the occlusal surfaces. An NIR-occlusal image shows opacities along the fissures where lesions due to caries are likely to be found; the white caps, on the other hand, appear transparent in the NIR-occlusal image. Similar behavior is observed on other teeth, namely, the high contrast between sound and demineralized enamel in the NIR, while areas with suspected fluorosis have

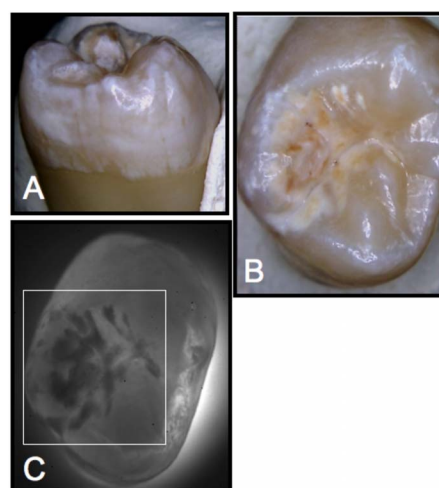


**Fig. 3** Visible reflected light images (a) and (b) and an NIR-occlusal image (c) of a tooth covered by mild fluorosis and likely caries and stains in the occlusal grooves. Note that areas of mild fluorosis along with the stains are not apparent in the NIR-occlusal image, while the areas likely to be caries (white box) are visible with high contrast.

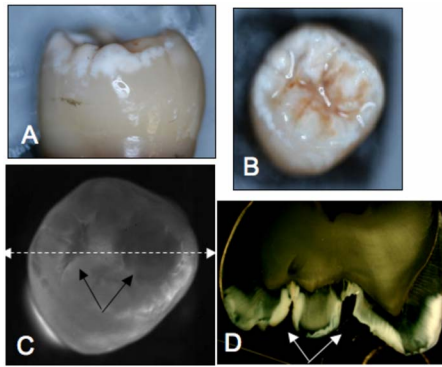


**Fig. 4** Visible reflected light images (a) and (b) and an NIR-occlusal image (c) of a tooth covered by mild fluorosis and either caries or more severe defects on the occlusal surface. Note that areas of mild fluorosis are not apparent in the NIR-occlusal image, while areas of more severe defects/caries are visible, as shown by the black arrows. The more severe areas of demineralization in the corresponding histological thin section (d) taken along the dotted line in (c) matches the more opaque areas of the NIR-occlusal image (white arrows).

slightly increased contrast or cannot be seen in the NIR. Many of the developmental defects appear transparent, while obvious caries appear opaque in NIR light. In Fig. 4, we have a tooth in which the entire occlusal surface is completely covered by apparent hypomineralization, with white cusps or “snow caps” whiter than the surrounding sound enamel due to the increased porosity of the developmental defect. In the corresponding NIR image, Fig. 4(c), most of the cusps still appear whiter than the surrounding sound enamel; however,

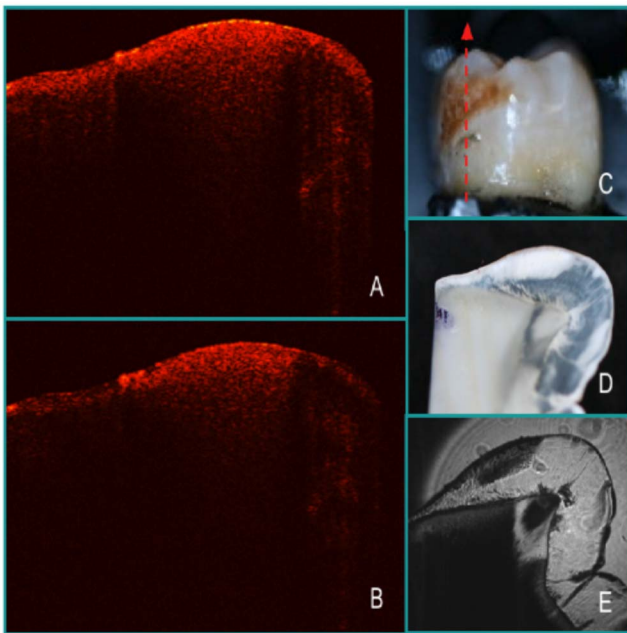


**Fig. 5** PS-OCT parallel ( $\parallel$ -axis) image (a) and orthogonal ( $\perp$ -axis) image (b) are shown along with the visible reflected light image (c) with a more serious defect. Visible (d) and near-IR (e) images of the histological thin section cut in the same position of the PS-OCT taken along the dotted line and arrow of (c) are also shown. (Color online only.)

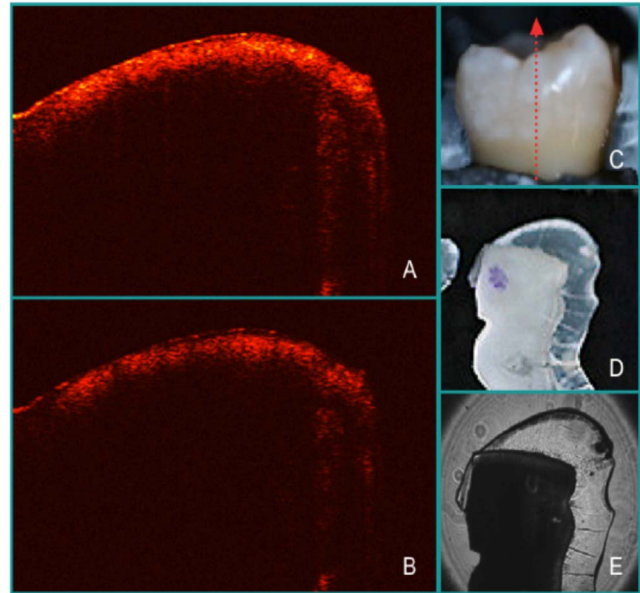


**Fig. 6** PS-OCT parallel ( $\parallel$ -axis) image (a) and orthogonal ( $\perp$ -axis) image (b) are shown along with the visible reflected light image (c) of a tooth with a shallow defect. More intense areas of reflectivity are yellow and red in the false-color PS-OCT images. Visible (d) and near-IR (e) images of the histological thin section cut in the same position of the PS-OCT taken along the dotted line and arrow of (c) are also shown. The defect appears whiter in the visible (d) and darker in the near-IR (e) images of the thin section; it is located on the top of the section and runs from the dentinal enamel junction to the cusp. (Color online only.)

there are two areas on the occlusal surface that appear more opaque than the surrounding enamel. The tooth was sectioned along the dotted line shown in Fig. 4(c), and the section is shown in Fig. 4(d). Most of the hypomineralization is localized to the enamel surface, with the exception of two large areas indicated by the two arrows where the decay or defect penetrates all the way through the enamel to the dentin. Those deeply penetrating areas of the defects/decay match the opacities in the NIR-occlusal images quite well. The differences in appearance appear to be related to the depth or severity of the developmental defect or caries lesion, the location on the tooth, and the imaging geometry.

### 3.2 PS-OCT Scans of Developmental Defects

PS-OCT was used to scan suspected sites of developmental defects on several teeth. Namely, white areas on smooth facial surfaces and cusps where demineralization due to caries is seldom found were chosen. Images of suspected developmental defects on two teeth are shown in Figs. 5 and 6, along with reflected light images and NIR-trans images of thin sections corresponding to the area scanned using the PS-OCT system. There are two images for each OCT scan. One corresponds to the light reflected in the same polarization state as the incident linearly polarized light ( $\parallel$ -axis), while the second image corresponds to the light reflected in the orthogonal or perpendicular polarization state ( $\perp$ -axis). Birefringence and depolarization from strong scattering such as that caused by demineralization in caries lesions or the porosity of developmental defects cause increased intensity in the perpendicular

polarization state ( $\perp$ ) versus the reflectivity in the original polarization ( $\parallel$ ). Moreover, the strong reflection at the tooth surface that prevents resolution of the structure of the defect near the enamel surface does not depolarize the incident light, so it is easier to resolve the structural differences in the defect in the orthogonal polarization image, the  $\perp$ -axis image. The red-dashed line across the smooth surface of the tooth shows the scan direction. The reflected intensity reading for each point (measured in dB), is shown from black to red to yellow, with yellow as the most intense reflectivity. The PS-OCT scan in Fig. 6 shows a shallow defect localized to the outer layer of enamel. This developmental defect is fairly uniform across the entire tooth surface, in contrast to a caries lesion, which is typically more localized. The areas of greater intensity in the PS-OCT images match the areas of the defect shown in the visible and NIR images of the histological thin sections of Figs. 6(d) and 6(e) very well. The  $\perp$ -axis PS-OCT image, Fig. 6(b), shows a thin transparent zone just below the enamel surface. This zone is indicative of a zone of higher mineral content above the body of the defect similar to what is observed after remineralization of caries lesions. That zone is also very apparent in the NIR-trans image of the thin section while it is very difficult to resolve in the visible light image of the thin section, Fig. 6(d) or the  $\parallel$ -axis PS-OCT image, Fig. 6(a). Similar behavior is observed for the more severe defect shown in Fig. 5. The PS-OCT images match the position, depth, and severity of the defects shown in the thin sections quite well, indicating that PS-OCT can be used to measure the depth and severity of the defects due to the increased light scattering from the increased porosity. A surface zone is also found in the more severe defect shown in Fig. 5, and that zone is clearly resolved only in the  $\perp$ -axis PS-OCT and the NIR-trans images.

### 3.3 Optical Properties of Developmental Defects

In order to determine whether there are fundamental differences in the nature of light scattering between hypomineralization due to developmental defects such as fluorosis and demineralization by caries, the optical attenuation of suspected defects of varying severity or mineral content was measured at 1310 nm in the near-IR. Near-IR images and x-ray microradiographs were acquired of thin tooth sections with mild to moderate developmental defects for comparison. The attenuation coefficients or scattering coefficients were acquired from the NIR images by measuring the attenuation of NIR light through 200- $\mu\text{m}$ -thick sections cut through the developmental defects. Absorption at this wavelength was assumed to be negligible. Each NIR image was processed by converting from relative intensity values to values of attenuation ( $\mu_r$ ) in units of inverse centimeters. The volume percent mineral content of each microradiography image was determined from a calibration curve of x-ray intensity versus the sample thickness of sound enamel sections. Line profiles through defect areas on 10 samples were selected, and 10 points from each sample of varying mineral content were plotted on a graph. A plot of the optical attenuation versus volume percent mineral loss was assembled from all the line profiles and is shown in Fig. 7. Points from each independent sample manifest similar behavior with mineral loss. Nonlinear regression using an exponential growth curve shows that the

optical scattering increases exponentially with mineral loss and that the magnitude of light scattering approaches a maximum after 10% mineral loss.

## 4 Discussion

It is clear that the increased porosity of developmental defects causes increased light scattering and increased attenuation in the NIR; therefore, such defects are readily detected by NIR imaging and PS-OCT at 1310 nm. However, many developmental defects did appear differently in NIR images in comparison with caries lesions on the same tooth. Based on our measurements, we believe that this perceived difference is due to the mild severity of most defects versus the more severe demineralization typical of caries lesions. The results are not surprising, since they appear similar in microradiographs and polarized light microscopy, and it is not possible to definitively differentiate the two with certainty. One can only assume a defect/lesion is one or the other based on location on the tooth. Differences in appearance are likely due to varying depth and severity of the developmental defect or caries lesion, the location on the tooth, and the imaging geometry. Although the magnitude of optical attenuation in developmental defects was measured to be less than that measured for dental caries<sup>12</sup> for similar mineral content, the difference was not significant enough to suggest that the differences could be easily exploited for clinical use for the differentiation between hypomineralization due to fluorosis and demineralization by caries.<sup>21,26</sup> Differences in scattering anisotropy or absorption were not investigated in this study, and there may be differences; however, such differences would also be difficult to exploit for clinical imaging.

The ability to differentiate shallow caries lesions/defects from deeper, more severe lesions/defects suggests that multi-spectral and multimodal NIR imaging can enhance the ability to assess lesion depth and severity. In a related unpublished study, we created shallow, artificial "white spot" lesions on tooth buccal and occlusal surfaces after 2 days of demineralization using a lactic acid solution at a pH of 4.5 and compared modes of NIR-imaging along with visible methods and quantitative light fluorescence (473-nm excitation).<sup>27</sup> The highest contrast of the superficial demineralization on both buccal and occlusal surfaces was achieved using NIR cross-polarized reflectance images. Therefore, the reflected light images should provide additional information to complement the transillumination images. For example, if a defect/lesion is visible in the reflected light image but not visible in the transmitted light image, it is probably shallow, and if it is visible in both images, it is likely to be fairly deep.

PS-OCT is capable of measuring the depth of developmental defects nondestructively. Moreover, these results also suggest that PS-OCT may also be potentially used as a tool to quantify the severity of developmental defects in a similar manner to caries lesions. Previous methods of assessing developmental defects are qualitative and based on color and tooth morphology. The ability to measure the depth and severity of developmental defects can be beneficial when attempting to remove a lesion for aesthetic purposes or when evaluating whether such defects can be remineralized. At this point, it is not clear whether PS-OCT will be able to easily differentiate caries from developmental defects, although the

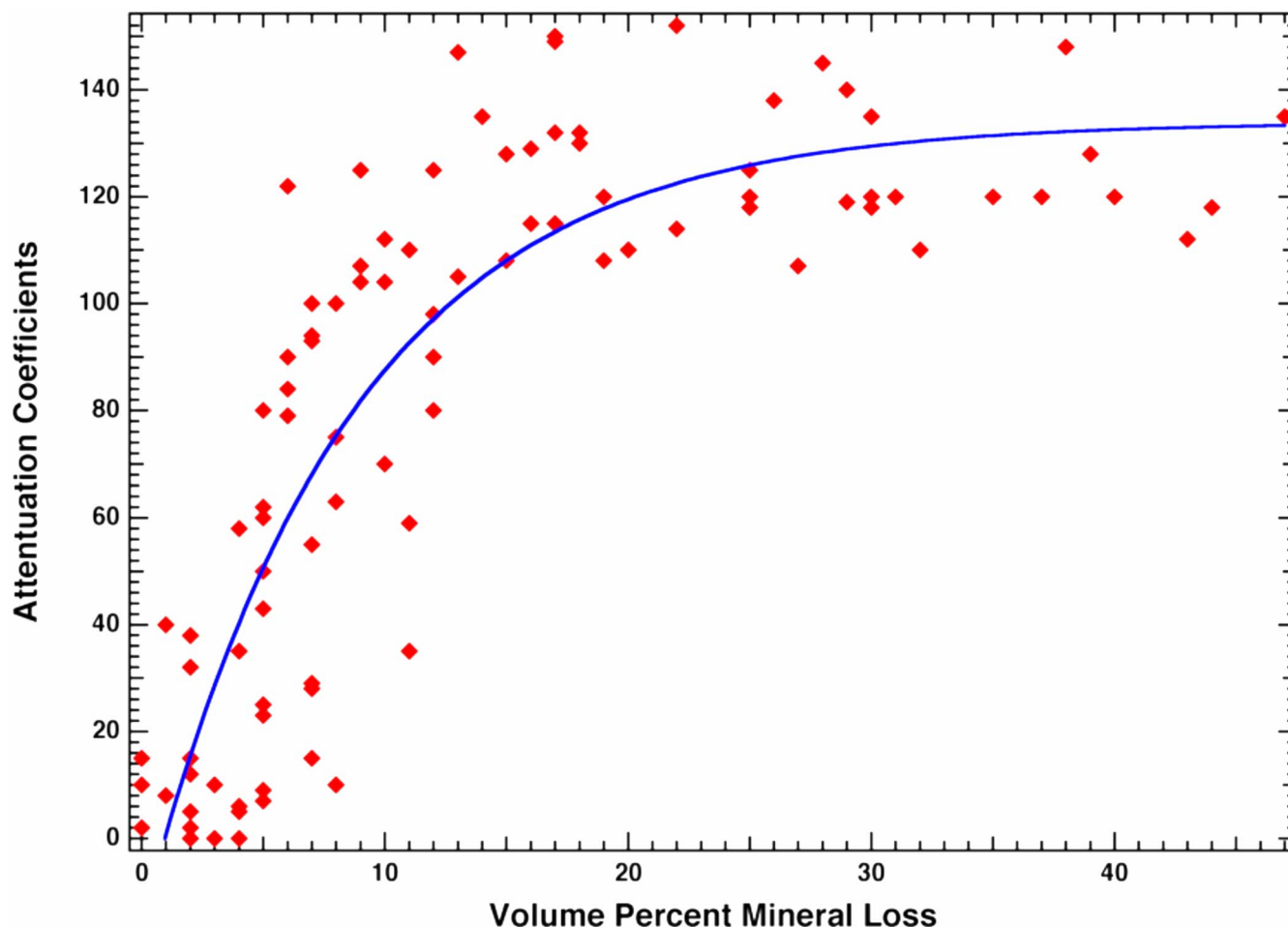


Fig. 7 A plot of the optical attenuation ( $\text{cm}^{-1}$ ) of 100 points taken from 10 tooth sections ( $200\text{-}\mu\text{m}$  thick) with developmental defects of varying severity (10 points per sample). The solid line represents the best exponential fit  $r^2=0.75$  to the attenuation coefficients versus volume percent.

overall geometry of the defects appear to be different from caries appearing more uniform over a large area such as the defect shown in Fig. 4. It is unlikely that a lesion due to caries would occur over a uniform depth across such a large area. PS-OCT can also be used to measure the structure of developmental defects, including the presence of the very important surface layer of higher mineral content.<sup>28,29</sup> This capability alone may enable the successful differentiation between inactive developmental defects and arrested (remineralized) lesions due to caries versus those lesions that are active and progressing. Only the active lesions due to caries should require intervention. Since quantitative light fluorescence (QLF) is being used for imaging early caries lesions and developmental defects,<sup>30-34</sup> it is appropriate to compare QLF with PS-OCT and NIR imaging. It has been demonstrated that the QLF signal and the loss of optical penetration measured using a conventional OCT system correlate well for early demineralization.<sup>35</sup> This is not surprising since both measurements reflect the overall magnitude of light scattering by the lesion. The most obvious advantage of PS-OCT is the ability to provide depth-resolved images of lesions/defects in addition to providing a quantitative measure of their severity. NIR imaging can be applied in reflectance mode, providing similar information to QLF. However, it has the advantage of being

applied in other transillumination modes, as presented in this paper, that exploit the high transparency of the enamel. Multimodal NIR imaging can potentially provide a measure of the depth and severity of the lesions and aids in discriminating between mild fluorosis and deeper, more penetrating caries lesions.

Both PS-OCT and NIR imaging methods are intended for independent use. While PS-OCT has the ability to provide depth-resolved images of lesions/defects and can be used to quantify the lesion severity by integration of the reflectivity with depth, it is more difficult to interpret and in the present configuration does not provide images of the entire tooth surface. However, that limitation will soon be eliminated with the introduction of frequency-domain-based fast-scanning methods capable of acquiring real-time OCT images over large areas of the tooth. NIR imaging is rapid, straightforward, and easy to interpret, but it does not provide direct depth-resolved information.

In conclusion, at first glance, many of our NIR images suggest that hypomineralization due to developmental defects such as fluorosis and demineralization by caries have very different optical behavior in the NIR at  $1310\text{ nm}$ . However, a more thorough examination shows that much of that differ-

ence can be attributed to the geometrical location of the defects on the teeth and the severity of the defect or caries lesion. These preliminary measurements on several teeth containing developmental defects and caries lesions suggest that NIR imaging and PS-OCT can provide valuable information relating to the depth and the severity of developmental defects in a similar manner that these tools can aid in the diagnosis of dental caries.

### Acknowledgments

This work was supported by NIH Grant Nos. T32-HDO52275-01, R01-DE17869, and R01-DE14698.

### References

- O. Fejerskov and E. Kidd, Eds., *Dental Caries: The Disease and Its Clinical Management*, Blackwell, Oxford, England (2003).
- E. D. Beltran-Aguilar, L. K. Barker, M. T. Canto, B. A. Dye, B. F. Gooch, S. O. Griffin, J. Hyman, F. Jaramillo, A. Kingman, R. Nowjack-Raymer, R. H. Selwitz, and T. Wu, "Surveillance for dental caries, dental sealants, tooth retention, edentulism, and enamel fluorosis—United States, 1988–1994 and 1999–2000," *MMWR Surveill Summ* **54**, 1–43 (2005).
- M. S. McDonagh, P. F. Whiting, P. M. Wilson, A. J. Sutton, I. Chestnutt, J. Cooper, K. Misso, M. Bradley, E. Treasure, and J. Kleijnen, "Systematic review of water fluoridation," *Br. Med. J.* **321**, 855–859 (2000).
- B. Angmar-Mansson, E. de Josselin de Jong, F. Sundstrom, and J. J. ten Bosch, "Strategies for improving the assessment of dental fluorosis: focus on optical techniques," *Adv. Dent. Res.* **8**, 75–79 (1994).
- S. M. Li, J. Zou, Z. Wang, J. T. Wright, and Y. Zhang, "Quantitative assessment of enamel hypomineralization by KaVo DIAGNOdent at different sites on first permanent molars of children in China," *Pediatr. Dent.* **25**, 485–490 (2003).
- G. Jones, R. S. Jones, and D. Fried, "Transillumination of interproximal caries lesions with 830-nm light," *Proc. SPIE* **5313**, 17–22 (2004).
- R. S. Jones, M. Staninec, and D. Fried, "Imaging artificial secondary caries under composite sealants and restorations," *Proc. SPIE* **5313**, 7–16 (2004).
- C. M. Bühler, P. Ngaothepitak, and D. Fried, "Imaging of occlusal dental caries (decay) with near-IR light at 1310-nm," *Proc. SPIE* **5687**, 125–131 (2005).
- D. Fried, J. D. B. Featherstone, R. E. Glana, and W. Seka, "The nature of light scattering in dental enamel and dentin at visible and near-IR wavelengths," *Appl. Opt.* **34**, 1278–1285 (1995).
- R. S. Jones and D. Fried, "Attenuation of 1310-nm and 1550-nm laser light through sound dental enamel," *Proc. SPIE* **4610**, 187–190 (2002).
- C. L. Darling and D. Fried, "Optical properties of natural caries lesions in dental enamel at 1310-nm," *Proc. SPIE* **5687**, 34–41 (2005).
- C. L. Darling, G. D. Huynh, and D. Fried, "Light scattering properties of natural and artificially demineralized dental enamel at 1310-nm," *J. Biomed. Opt.* **11**, 034023 (2006).
- D. Fried, J. D. B. Featherstone, C. L. Darling, R. S. Jones, P. Ngaothepitak, and C. M. Buehler, Eds., *Early Caries Imaging and Monitoring with Near-IR Light*, Vol. **49**, W. B. Saunders Company, Philadelphia (2005).
- B. E. Bouma and G. J. Tearney Eds., *Handbook of Optical Coherence Tomography*, Marcel Dekker, New York (2002).
- B. T. Amaechi, S. M. Higham, A. G. Podoleanu, J. A. Rogers, and D. A. Jackson, "Use of optical coherence tomography for assessment of dental caries: quantitative procedure," *J. Oral Rehabil.* **28**, 1092–1093 (2001).
- B. Colston, M. Everett, L. Da Silva, L. Otis, P. Stroeve, and H. Nathel, "Imaging of hard and soft tissue structure in the oral cavity by optical coherence tomography," *Appl. Opt.* **37**, 3582–3585 (1998).
- B. W. Colston, U. S. Sathyam, L. B. DaSilva, M. J. Everett, and P. Stroeve, "Dental OCT," *Opt. Express* **3**, 230–238 (1998).
- F. I. Feldchtein, G. V. Gelikonov, V. M. Gelikonov, R. R. Iksanov, R. V. Kuranov, A. M. Sergeev, N. D. Gladkova, M. N. Ourutina, J. A. Warren, and D. H. Reitze, "In vivo OCT imaging of hard and soft tissue of the oral cavity," *Opt. Express* **3**, 239–251 (1998).
- M. J. Everett, B. W. Colston, U. S. Sathyam, L. B. D. Silva, D. Fried, and J. D. B. Featherstone, "Non-invasive diagnosis of early caries with polarization sensitive optical coherence tomography (PS-OCT)," *Proc. SPIE* **3593**, 177–183 (1999).
- A. Baumgartner, S. Dicht, C. K. Hitzberger, H. Sattmann, B. Robi, A. Moritz, W. Sperr, and A. F. Fercher, "Polarization-sensitive optical coherence tomography of dental structures," *Caries Res.* **34**, 59–69 (2000).
- D. Fried, J. Xie, S. Shafi, J. D. B. Featherstone, T. Breunig, and C. Q. Lee, "Early detection of dental caries and lesion progression with polarization sensitive optical coherence tomography," *J. Biomed. Opt.* **7**, 618–627 (2002).
- R. S. Jones, G. D. Huynh, G. C. Jones, and D. Fried, "Near-IR transillumination at 1310-nm for the imaging of early dental caries," *Opt. Express* **11**, 2259–2265 (2003).
- C. M. Bühler, P. Ngaothepitak, and D. Fried, "Imaging of occlusal dental caries (decay) with near-IR light at 1310-nm," *Opt. Express* **13**, 573–582 (2005).
- P. Ngaothepitak, C. L. Darling, and D. Fried, "PS-OCT of occlusal and interproximal caries lesions viewed from occlusal surfaces," *Proc. SPIE* **6137**, 61370L (2006).
- J. Bush, P. Davis, and M. A. Marcus, "All-fiber optic coherence domain interferometric techniques," *Proc. SPIE* **4204**, 71–80 (2000).
- R. S. Jones and D. Fried, "Quantifying the remineralization of artificial caries lesions using PS-OCT," *Proc. SPIE* **6137**, 613708 (2006).
- J. Wu, "Detection of white spot lesions with near-IR imaging," MS Thesis, Univ. of California, San Francisco (2008).
- R. S. Jones and D. Fried, "Remineralization of enamel caries can decrease optical reflectivity," *J. Dent. Res.* **85**, 804–808 (2006).
- R. S. Jones, C. L. Darling, J. D. B. Featherstone, and D. Fried, "Remineralization of *in vitro* dental caries assessed with polarization sensitive optical coherence tomography," *J. Biomed. Opt.* **11**, 014016 (2006).
- U. Hafstroem-Bjoerkman, E. de Josselin de Jong, A. Oliveby, and B. Angmar-Mansson, "Comparison of laser fluorescence and longitudinal microradiography for quantitative assessment of *in vitro* enamel caries," *Caries Res.* **26**, 241–247 (1992).
- M. Ando, A. F. Hall, G. J. Eckert, B. R. Schemehorn, M. Analoui, and G. K. Stookey, "Relative ability of laser fluorescence techniques to quantitate early mineral loss *in vitro*," *Caries Res.* **31**, 125–131 (1997).
- S. Tranaeus, S. Al-Khateeb, S. Bjorkman, S. Twetman, and B. Angmar-Mansson, "Application of quantitative light-induced fluorescence to monitor incipient lesions in caries-active children. A comparative study of remineralisation by fluoride varnish and professional cleaning," *Eur. J. Oral Sci.* **109**, 71–75 (2001).
- J. J. ten Bosch, "Summary of research of quantitative light fluorescence," in *Early Detection of Dental Caries II*, Vol. **4**, pp. 261–278, G. K. Stookey, Ed., Indiana University, Indianapolis (1999).
- G. K. Stookey and C. Gonzalez-Cabezas, "Emerging methods of caries diagnosis," *J. Dent. Educ.* **65**, 1001–1006 (2001).
- B. T. Amaechi, A. Podoleanu, S. M. Higham, and D. A. Jackson, "Correlation of quantitative light-induced fluorescence and optical coherence tomography applied for detection and quantification of early dental caries," *J. Biomed. Opt.* **8**, 642–647 (2003).